Eur. Phys. J. B **42**, 573–580 (2004)
DOI: 10.1140/epjb/e2005-00017-7

THE EUROPEAN PHYSICAL JOURNAL B

An analytical approach to neuronal connectivity

L. da F. Costa and M.S. Barbosa[a]

Cybernetic Vision Research Group, GII-IFSC, Universidade de São Paulo, São Carlos, SP, Caixa Postal 369, 13560-970, Brasil

Received 28 July 2004
Published online 18 January 2005 –

Abstract. This paper describes how to analytically characterize the connectivity of neuromorphic networks taking into account the morphology of their elements. By assuming that all neurons have the same shape and are regularly distributed along a two-dimensional orthogonal lattice with parameter Δ, we obtain the exact number of connections and cycles of any length by applying convolutions and the respective spectral density derived from the adjacency matrix. It is shown that neuronal shape plays an important role in defining the spatial distribution of synapses in neuronal networks. In addition, we observe that neuromorphic networks typically present an interesting property where the pattern of connections is progressively shifted along the spatial domain for increasing connection lengths. This arises from the fact that the axon reference point usually does not coincide with the cell center of mass of neurons. Morphological measurements for characterization of the spatial distribution of connections, including the adjacency matrix spectral density and the lacunarity of the connections, are suggested and illustrated. We also show that Hopfield networks with connectivity defined by different neuronal morphologies, which are quantified by the analytical approach proposed herein, lead to distinct performances for associative recall, as measured by the overlap index. The potential of our approach is illustrated for digital images of real neuronal cells.

PACS. 89.75.Fb Structures and organization in complex systems – 87.18.Sn Neural networks – 02.10.Ox Combinatorics; graph theory

1 Introduction

A particularly meaningful way to understand neurons is as cells optimized for *selective connections*, i.e. they connect to each other in a way as to achieve proper circuitry and behavior. Indeed, the intricate shape of dendritic and axonal trees provides a means for connecting with specific targets while minimizing both the cell volume and its metabolism (e.g. [1,2]). Great attention has been placed on the importance of synaptic strength over the emerging neuronal behavior. On the other hand, geometrical features, such as the shape and spatial distribution of the involved neurons, are closely related to the network connectivity. In addition, the topographical organization and connections pervading the mammals' cortex provide further indication that adjacencies and spatial relationships are fundamental for information processing by biological neuronal networks. The importance of neuronal geometry has been reflected by the growing number of related works (see, for instance, [3]). However, most of such approaches target the characterization of neuronal morphology in terms of indirect and incomplete (i.e. degenerated) measurements such as area, perimeter and fractal dimension of the dendritic and axonal arborizations. Interesting experimental results regarding the connectivity of neuronal cells growth in vitro have been reported in [4,5] and what is possibly the first direct computational approach to neuronal connectivity was only recently reported in [6], where experimental estimation of the critical percolation density as neuronal cells were progressively superposed onto a two-dimensional domain. At the same time, recent advances in complex network formalism (e.g. [7–11]) provide a wealthy of concepts and tools for addressing connectivity. Initial applications of such a theory to bridge the gap between neuronal shape and function were reported in [12,13].

As the investigation of the relationship between neuronal shape and function is underlain by computational approaches involving numerical methods and simulation, a need arises to develop an analytical framework for neuromorphic characterization that could lead to additional insights and theoretical results regarding the relationship between neuronal shape and function. The present work describes an analytical approach capable of characterizing the connectivity of neuronal networks composed by repetitions along the space of the same neuron, taking into account explicitly the cell morphology. Such a kind of network can be considered as a "toy model" for biological neuronal systems characterized by a high degree of planarity, such as ganglion cell retinal mosaics [14],

[a] e-mail: marconi@if.sc.usp.br

Purkinje cells, and the basal dendritic arborization of cortical pyramidal cells. The extension of such a methodology to three-dimensional neuronal systems is conceptually straightforward but it will not be considered in the current work because of computational limitations. The underlying idea of the proposed analytical approach is to use the symmetries induced by the periodical boundary conditions in order to allow the connecting matrix describing the network to become a circulant matrix. Important features such as the number of connections and cycles can then be exactly obtained from the spectrum of this matrix. The morphological atributes of the spatial distribution of points, as characterized by the concept of Lacunarity[1], is also considered (see details in Sect. 3) as a complementary measurement of the connectivity pattern.

The effect of different neuronal shapes over the dynamics of the respective neuronal systems (Hopfield) built upon such connections is then investigated by using the proposed methodology. It is shown that neuronal shape not only plays an important role in defining the spatial distribution of synapses in neuronal networks, but also imposes critical constraints over the respective behavior.

2 Methodology

The analytical representation of the connectivity of a neuronal network results from the convolution of a function, which represents the neuronal cell, with Dirac deltas. The adopted basic construction is illustrated in Figure 1, where the convolution of the neuronal cell $g(x)$ in (b) with the Dirac delta $f(x)$ in (a) produces a copy of the original cell at the position of the delta (c). This can be mathematically expressed as

$$\delta(\boldsymbol{x}-\boldsymbol{a}) * g(\boldsymbol{x}) = g(\boldsymbol{x}-\boldsymbol{a}), \tag{1}$$

where the operation $*$ stands for the usual definition of the convolution integral between two images $u(\boldsymbol{r})$ and $v(\boldsymbol{r})$, i.e.

$$h(\boldsymbol{r}) = (u * v)(\boldsymbol{r}) = \int_0^{\boldsymbol{r}} u(\boldsymbol{\tau}) v(\boldsymbol{r}-\boldsymbol{\tau}) d\boldsymbol{\tau}. \tag{2}$$

Let the neuronal cell be represented in terms of the triple $\eta = [A, S, D]$ where A is the set of points belonging to its axonal arborization, S is the set of points corresponding to the respective soma (neuronal body) and D are the dendritic arborization points. For simplicity's sake, a finite and discrete neuronal model is considered prior to its continuous general formulation. We therefore assume that the points used to represent the neuron belong to the square orthogonal lattice $\Omega = \{1, 2, \ldots, N\} \times \{1, 2, \ldots, N\}$, with parameter $\Delta = 1$. Initially, the axon and soma are represented by a single point each. Such

[1] This quantity, which is inversely related to the degree of translational invariance of the analyzed patterns [15–19], is frequently applied in order to complement fractal dimension characterization.

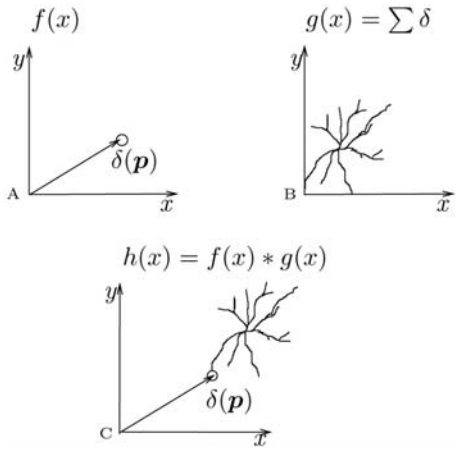

Fig. 1. The convolution of an axon function with a dendritic distribution.

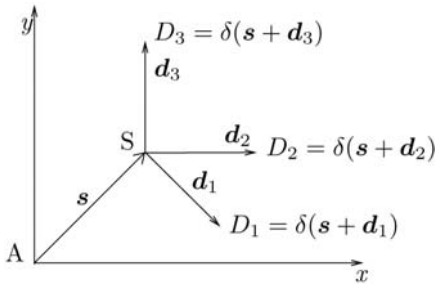

Fig. 2. The geometry of a simplified neuronal cell represented in terms of its axon A, soma centroid S and dendrite points D_i.

points could be understood as corresponding to the tip of the axon and the soma center of mass, respectively. The dendritic arborization is represented in terms of the finite set of dendrite points $D = D_1, D_2, \ldots, D_M$ and, in order to prevent loops, it is henceforth assumed that a dendrite point never coincides with the axon. Figure 2 illustrates such a geometrical representation for a neuron with 3 dendrite points. Observe that the coordinate origin coincides with the axon, which is taken as reference for the soma and dendrite coordinates, and the arrows refer to the relative positions of the soma and dendrites and not to the direction of signal transmission by a real neuronal cell, which occurs in the opposite direction (i.e. from dendrites to axon). Neuromorphic networks (actually digraphs [8]) can now be obtained by placing one such a neuron at all possible nodes of the orthogonal lattice Ω.

A connection is established whenever an axon is overlaid onto a dendrite point. The resulting connection pattern stands out as a particularly important feature of the obtained network, as it defines the possible communications between the cells. Thus, it is important to derive analytical expressions which describe the respective neuronal connectivity, e.g. by considering the spatial distribution of paths and cycles of any specific length along the network.

We start by considering the connections with a single specific neuron i placed with its axon at position $\boldsymbol{p}$, illustrated in Figure 3 together with four other neuronal cells

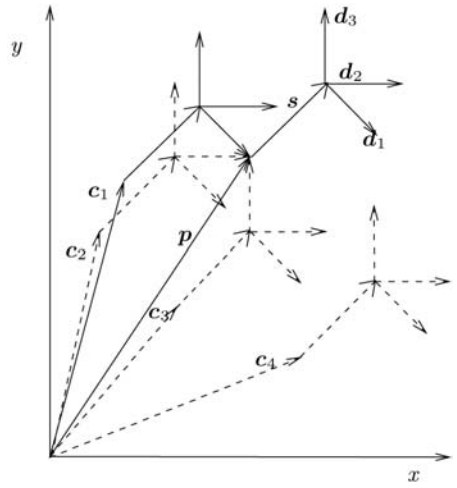

Fig. 3. The neurons connected through unit-length paths to neuron i which is placed with its axon A at $\boldsymbol{p}$ can be obtained through the convolution between the position $\delta(\boldsymbol{p})$ of neuron i with the function representing the dendritic structure.

at positions $\boldsymbol{c_1}$, $\boldsymbol{c_2}$, $\boldsymbol{c_3}$ and $\boldsymbol{c_4}$. Given the particular geometry of the basic cell, three connections are implied with the cells at $\boldsymbol{c_1}$, $\boldsymbol{c_2}$ and $\boldsymbol{c_3}$ whose dendrites coincide with the axon of the cell i. For cell $\boldsymbol{c_1}$, this situation can be mathematically expressed as $\boldsymbol{c_1} = \boldsymbol{p} - \boldsymbol{d_1} - \boldsymbol{s}$. The fourth cell $\boldsymbol{c_4}$ illustrates one of the many neurons which are *not* connected to cell i.

Two directly connected cells, as described above, are henceforth represented as two nodes connected by a unit-length path (a simple arc) of a respectively associated directed graph. As is clear from this construction, the set of neurons connected to i through unit-length paths can be obtained by convolving the initial point[2] $\delta(\boldsymbol{p})$ (the tip of the axon), and the function $g(x, y)$ represents the neuronal cell, i.e.

$$g(x,y) = \delta(-\boldsymbol{d_1} - \boldsymbol{s}) + \delta(-\boldsymbol{d_2} - \boldsymbol{s}) + \delta(-\boldsymbol{d_3} - \boldsymbol{s}), \quad (3)$$

where the minus signs mean that the function representing the cell shape can be flipped along both axes, so as to obtain adequate propagation of the connections, i.e. from the axon to the dendrites. For instance, in Figure 3, the propagation of information proceeds from the original axon at $\boldsymbol{p}$ to the dendrites at $\boldsymbol{c_1}$, $\boldsymbol{c_2}$, and $\boldsymbol{c_3}$.

More generally, given a set of initial neurons with axons represented as a sum of Dirac deltas $\xi(x, y)$, the density of dendrites connected to those neurons by unit-path lengths can be obtained from equation (4). Observe that $\chi(x, y)$ may contain Dirac deltas with intensities larger than one, resulting from sums of coinciding deltas. The function $\nu(x, y)$ in equation (5) is analogous to $\chi(x, y)$ but here all Dirac deltas in that function are replaced by unit Dirac deltas. Such a procedure is required in order to take into account the restriction that only one synapsis can be established at each point along the 2D dendrites.

[2] Unless mentioned otherwise, we use a simplified notation for the Dirac delta function $\delta(x - a) = \delta(a)$.

The above formulation can be easily extended to higher orders of path lengths. The function expressing the density of the dendrites connected to the original neurons through paths of length k (see footnote[3]) is given by equation (6). Equation (7) is a generalization of equation (5). The number of connections with length k is quantified by equation (8), which can be used as an additional feature for characterizing the connectivity of the obtained networks. Observe that the use of the Dirac delta function in such a formulation allows the immediate extension of such results to continuous spatial domains.

$$\chi(x,y) = g(x,y) * \xi(x,y) \quad (4)$$

$$\nu(x,y) = \begin{cases} \delta(x,y) & if \quad \chi(x,y) \neq 0 \\ 0 & otherwise. \end{cases} \quad (5)$$

$$\chi_k(x,y) = \underbrace{g(x,y) * \ldots * g(x,y)}_{k\times} \xi(x,y) \quad (6)$$

$$\nu_k(x,y) = \begin{cases} \delta(x,y) & if \quad \chi_k(x,y) \neq 0 \\ 0 & otherwise. \end{cases} \quad (7)$$

$$\tau_k(x,y) = \sum_{j=1}^{k} (\nu_j(x,y)). \quad (8)$$

While the analytical characterization of the connectivity of the considered network model has been allowed by the fact that identical neuronal shapes are distributed along all points of the orthogonal lattice, it is interesting to consider extensions of such an approach to other situations. For example, we can consider sparser configurations, characterized by a larger lattice parameter Δ. Such an extension involves sampling the neuronal cell image at larger steps. Figure 4 shows two digital images[4], obtained from real ganglion cells, (a) and (b), and their respective functions $\chi_k(x, y)$ (given by Eq. (6)) for $k = 2$ and 3. The axon has been placed over the centroid of the neuronal shape (including soma and dendrites), whereas the dendritic trees have been spatially sampled into 2033 and 671 pixels, respectively. Figure 5 shows $\chi_k(x, y)$ obtained for the cell in Figure 4a but with the soma located at the cell center of mass, which is displaced from the cell centroid by $\boldsymbol{s} = (0, 7)$ pixels. It should be observed that retinal ganglion cells do not synapse one another, rather they project outside the retina (the optic nerve). However, as they are mostly planar, such a type of neuron provides a particularly suitable illustration of the proposed methodology.

The effect of considering a more substantial axon (rather than a single point) is illustrated in Figure 6 and formalized in equations (9–11). First, the original

[3] A path of length k between two nodes corresponds to a sequence of k connected edges found between those two nodes.

[4] The neuronal cell images in this figure and in the subsequent ones were adapted with permission from [14].

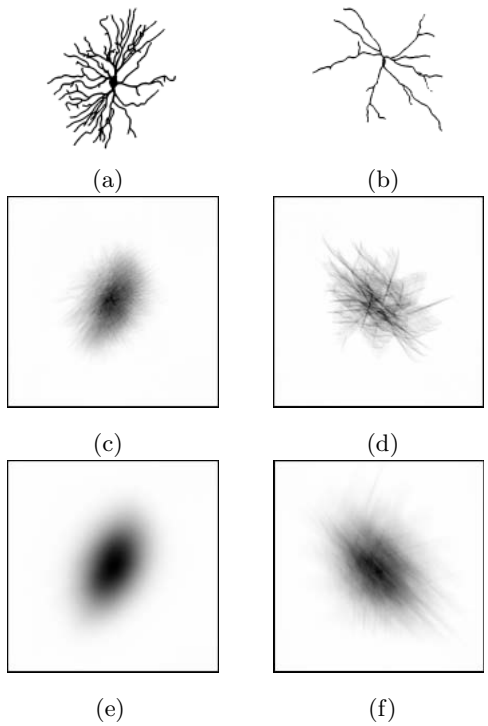

Fig. 4. Two real neuronal cells (a-b) and their respective total number of connections of length $k = 2$ (c-d) and 3 (e-f). The axon has been placed at the cell centroid (considering soma plus dendrites).

dendrites $d(x, y)$, represented in darker gray-level in Figure 6a, are convolved with the axon $a(x, y)$, represented in lighter gray-level in the same figure, in order to obtain the distribution $b(x, y)$ shown in Figure 6b and given by equation (9), which is subsequently thresholded in order to obtain a binary image $c(x, y)$ (i.e. an image composed of zeroes and ones) as given in equation (10) and displayed in Figure 6c. Such an image represents an enlarged target for connections with other cells, implied by the fact that the axon is no longer a point, but a generic shape. The distribution of connections $r(x, y)$ is finally obtained by convolving the image 6c with the dendrite profile, as expressed in equation (11) and illustrated in Figure 6d.

$$b(x, y) = d * a \tag{9}$$

$$c(x, y) = \begin{cases} 1 & if \quad b(x, y) > 0 \\ 0 & otherwise. \end{cases} \tag{10}$$

$$r(x, y) = d(x, y) * c(x, y). \tag{11}$$

Figure 7 shows the obtained distribution of synaptic connections as the axon is progressively extended. Clearly, the effect of the axon is to imply a broader dispersion of the connections that take into account its intrinsic shape. It should be noticed that, in reality, axons are frequently longer than dendrites in the same neuron, and also branch profusely. Therefore, the use of shorter axons in the above examples are mainly for the sake of a more effective graphical illustration.

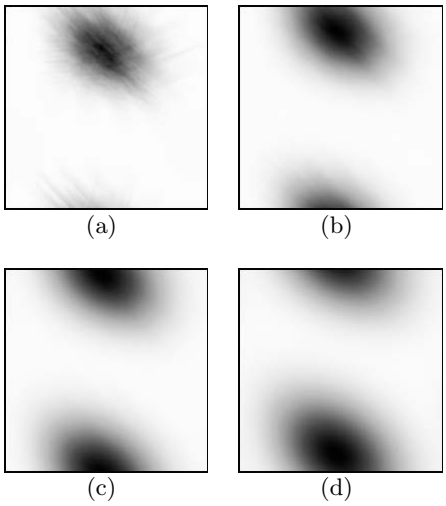

Fig. 5. The total number of connections of length $k = 1$ (a), 2 (b), 3 (c) and 4(d) for the neuronal cell in Figure 4a with the axon displaced from the cell centroid by $\boldsymbol{s} = (0, 7)$ pixels.

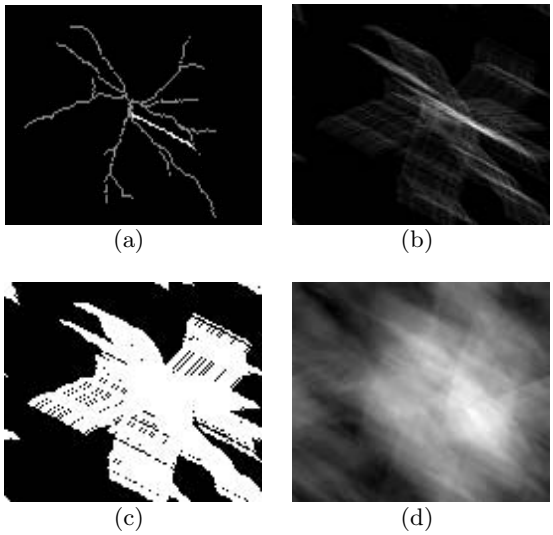

Fig. 6. Sequence of operations required in order to incorporate generic axonal shape, shown here in lighter gray, into the proposed approach: (a) original neuron; (b) the convolution between its axon and dendrites; (c) the thresholded version of such a convolution; and (d) the distribution of connections obtained by convolving the image in (c) with the dendrites in (a).

It is clear from such results that the neuronal morphology strongly determines the connectivity between cells in two important senses: (i) the spatial scattering of the dendrite points influences the connectivity distribution and (ii) the relative position of the axon defines how the centroid of the connections shifts for increasing values of k. While the increased number of synaptic connections implied by denser neuronal shapes is as expected, it is clear from the example in Figure 5 that the distance from the axon to the cell center of mass implies spatial displacement of the connection pattern. Given the predominantly

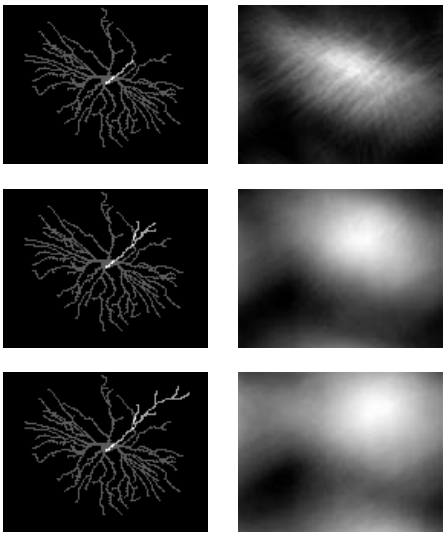

Fig. 7. The role of the axon (in light gray) in defining the connectivity pattern. The connection profile follows the change of the axon, moving toward the same direction.

two-dimensional structure of the mammals' cortex, such an effect provides an interesting means to transmit information horizontally along such structures. In other words, faster signal transmission along the cortical surface is achieved whenever the axon is placed further away from the dendritic tree. As the proper characterization, classification, analysis and simulation of neuromorphic networks are all affected by these two interesting phenomena, it is important to derive objective related measurements. The next section addresses the characterization of the morphology of such networks.

3 Morphology

Let $P_k(x, y)$ be a density function obtained by normalizing $\chi_k(x, y)$, i.e.

$$P_k(x, y) = \frac{\chi_k(x, y)}{\int_{-\infty}^{\infty} \chi_k(x, y) dx dy}. \quad (12)$$

The spatial scattering of the connections can be quantified in terms of the respective covariance matrix K_k [20] of the scalar field $P_k(x, y)$, and the spatial displacement of the centroid of $P_k(x, y)$ can be quantified in terms of the 'speed' magnitude $v = ||\boldsymbol{s}||$. Additional geometrical measurements of the evolution of the neuronal connectivity that can be derived from the covariance matrix K_k include the angle α_k that the distribution main axis makes with the x-axis and the ratio ρ_k between the largest and smallest respective eigenvalues.

Additional information about the morphological properties of the connections implied by the geometry of the individual cells can be obtained from the respective adjacency matrix A, which represents the existing connections between the cells. Figure 8 illustrates the steps required in order to obtain matrix A. First, the original cell is represented as a matrix as shown in Figure 8a, which is subsequently rearranged as a row vector as shown in Figure 8b. The mathematical description of this operation is given by

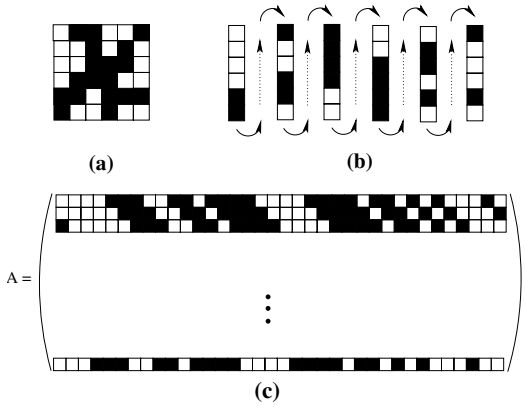

Fig. 8. The procedure to build the adjacency matrix A from the shape of the neuronal cell. (a) A prototypical neuron represented as a matrix, M. (b) The rearrangement scheme and (c) the circulant matrix A, where a black square means value 1 and a white square indicates value 0.

$$A(1, j) = M(mod(j - 1, N) + 1, \lfloor j/n \rfloor + 1). \quad (13)$$

The first row of matrix A is now obtained by copying the resulting vector shown in Figure 8b. The remaining rows of A are obtained by circulating the first line along the matrix, as shown in Figure 8c. As a consequence, A becomes a circulant matrix.

An interesting network feature related to connectivity is its number $C_{\ell,k}$ of cycles of length ℓ established by the synaptic connections, which can be obtained from the diagonal of the integer powers of the adjacency matrix A. The N^2 eigenvalues of the thus obtained *adjacency matrix* [7] of the whole two-dimensional network are henceforth represented as λ_i, $i = 1, 2, \ldots, N^2$. As A is circulant, these eigenvalues can be immediately obtained from the Fourier transform of its first row. Observe that the simplicity and speed of such an approach allow for systematic investigation of a variety of different neuronal shapes. As the cell reference point is assumed never to coincide with a dendrite point, we also have that $\sum_{r=1}^{N} \lambda_r = 0$. As A is a non-negative matrix, there will always be a non-negative eigenvalue λ_M, called the *dominant eigenvalue of* A, such that $\lambda_r \leq \lambda_M$ for any $r = 1, 2, \ldots, N$. The *spectral density* (e.g. [7]) of the adjacency matrix, defined as

$$\rho(\lambda) = \frac{1}{N} \sum_{r=1}^{N} \delta(\lambda - \lambda_r), \quad (14)$$

where λ_p is the pth eigenvalue of A, provides an additional way to characterize the topology of the obtained networks.

The eigenvalue λ_M, which depends on the specific dynamics through which new edges are incorporated into the network, represents an interesting parameter for characterizing the cyclic composition of complex networks. Figures 9a and b show the real part (recall that the adjacency

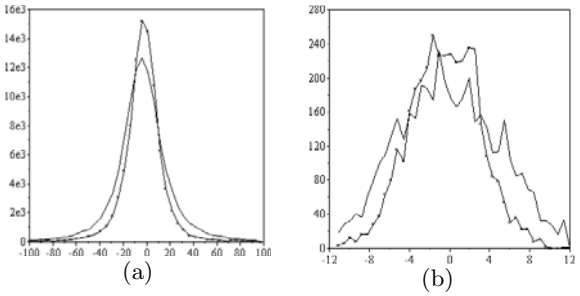

Fig. 9. Spectral density of the adjacency matrices obtained for the neuronal cells in Figure 4 considering $\Delta = 1$ (a) and $\Delta = 5$ (b). The crossed lines refer to the sparser neuronal cell.

matrix for a digraph is not necessarily symmetric) of the spectral density of the adjacency matrices obtained for the neuronal cells in Figures 4a and b considering lattice spacings $\Delta = 1$ and 5. The wider dispersion of the spectrum of the denser cell in Figure 9a reflects a higher potential for connections of that neuron in both cases. It is also clear that the separation of cells by $\Delta = 5$ leads to a substantially smaller spectrum, with immediate implications for the respective neuronal connectivity.

An additional morphological property of the spatial distribution of the connections is their respective *lacunarity* (e.g. [19]), which expresses the degree of translational invariance of the obtained densities. Therefore, lower values of lacunarity indicate that the analysed patterns (in our case the synapses) are more uniformly distributed along the considered space. An opposite effect is observed for higher lacunarity values. All in all, a neuronal cell exhibiting high lacunarity tends to be characterized by a more uniform pattern of synapses with other neighboring cells. This functional may be calculated by moving a window of a given radius r centered at (x, y) throughout the whole image as the number $N(r, x, y)$ of object points that falls inside it are recorded. The standard deviation $\sigma(r)$ and the mean values $\mu(r)$ of $N(r, x, y)$, for each window size r, are used to calculate the lacunarity for the scale given by r through the formula

$$L(r) = \frac{\sigma(r)}{\mu(r)^2}. \tag{15}$$

Figure 10 shows the lacunarities of the connection densities obtained for the two considered cells with respect to $k = 1$ to 4. It is interesting to observe that most of the lacunarity differences are observed for $k = 1$, with similar curves being obtained for larger values of k. At the same time, the denser cell led to lower lacunarity values. Given their immediate implications for neuronal connectivity, the above proposed set of neuronal shape measurements present specially good potential for neuron characterization and classification.

4 Associative recall

One of the most important functional properties of Hopfield neuronal networks is their associative recall,

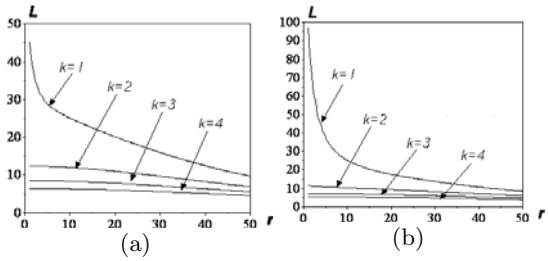

Fig. 10. Examples of lacunarity: (a) for the neuron in Figure 4a; (b) for the neuron in Figure 4b.

which can be quantified by the overlap measurement, obtained by comparing the originally trained and the recovered patterns. A Hopfield network is completely determined by its respective connecting matrix, which in the case of the models considered in the present work is constrained by the adjacency matrix derived from the morphological structure in the sense that only the weights corresponding to existing connections are allowed to vary [13]. Therefore, the shape of the neuron has a direct impact on the performance of the network, which is chiefly dictated by the null-space of the adjacency matrix spectrum [21]. The analytical approach introduced in the current work can be immediately used for the estimation of overlaps considering different neuronal shapes.

In the standard Hopfield setup the cells are either firing ($S_i = 1$) or silent ($S_i = -1$) and are updated according to the rule

$$S_i \rightarrow \text{sign}\left(\sum_k J_{ik} S_k\right) \tag{16}$$

with synaptic strengths $J_{ik} = \sum_\mu \xi_i^\mu \xi_k^\mu$ (Hebb rule) if i and k are connected, where $\xi_i^\mu = \pm 1$, $\mu = 1, 2, \ldots P$, are P random bit-strings called input patterns, and one of them, perturbed uniformly along its extent, is supposed to be recalled by this updating rule (i.e. associative memory). The quality of recall is measured by the overlap $\Psi = \sum_i S_i \xi_i^1$ if the first pattern is supposed to be recovered.

We consider the simple prototypical cell patterns presented in Figure 11. A network was obtained for each cell shape by using the above formalism, and a non-randomly diluted Hopfield model with such connection matrix was then implemented for the networks and serially repeated a hundred times to gain statistical significance. All three networks consist of 441 neurons and the memory model is set to recall 25 background patterns with 20 percent of noise. For efficiency's sake, the recovering stage stops whenever a stable point (or reasonable fixed limit) is reached. To incorporate the effect of changing the axons position, which is potential significant from the biological point of view, we perturbed the reference point of the axon randomly and gradually. This allowed us to study the robustness of the memory model.

Figure 12 shows the overlaps obtained while considering three simple neuronal shapes, namely the artificial

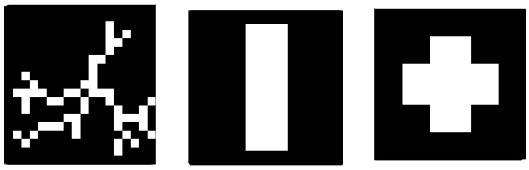

Fig. 11. Three prototypical cell shapes used in the morphological Hopfield simulation.

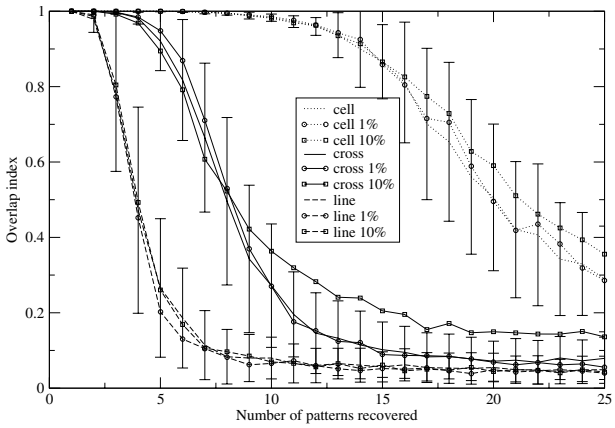

Fig. 12. The overlap curves for three different cell shapes shown in Figure 11.

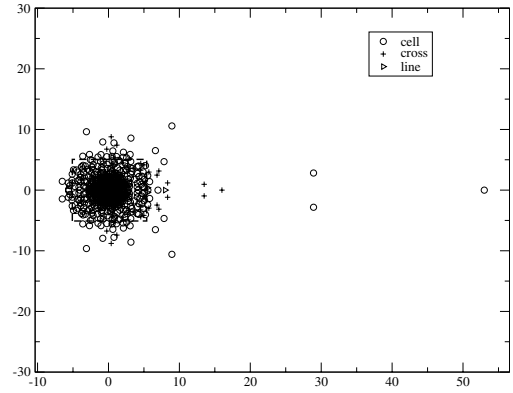

Fig. 13. The spectrum of the adjacency matrix A (represented in the complex plane) for the three different cell shapes shown in Figure 11, the marked inset is zoomed in Figure 14.

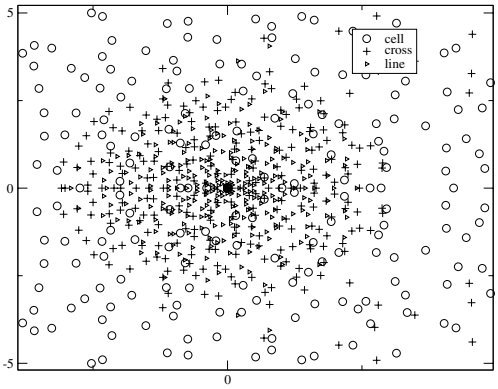

Fig. 14. The spectrum of the adjacency matrix A zoomed from the inset of Figure 13, showing the spread in the distribution of eigenvalues for the considered patterns.

neuronal cell, a line and a cross shown in Figure 11. Each of these shapes have the same area (i.e. number of pixels). For each cell pattern we have three overlap curves representing respectively: the lattice as it is, a perturbed version with one percent of uniform noise (in pixels), and another perturbed version with ten percent noise. Although the influence of such perturbations are masked by the stochastic nature of the system, we can see that as far the overlaps are taken as an indication of performance, the model is robust to network topology changes and sensitive to neuronal shape. An order clearly emerged in the overlaps albeit, as indicated by the large deviation, it is a visibly degenerated morphological measure. The more spatially distributed shapes tended to lead to better performance. The eigenvalues for each of the three considered cases are illustrated graphically in Figure 13. It is clear from this figure that the eigenvalues tend to organize symmetrically with respect to the real axis. Also, the eigenvalue dispersions obtained for the cases line, cross and cell tended to be progressively broader, reflecting their original spatial structure. In other words, shapes more uniform and isotropically distributed along space tended to produce broader eigenvalue distributions. The better overlap figures obtained for sparser patterns is closely related to the fact that more distributed eigenvalues are obtained in those cases, reducing the null space for memory representation.

5 Conclusions

An analytical approach to the characterization of neuronal connectivity was proposed and illustrated with respect to synthetic and real neurons. It was shown that the connections of progressive length established along the neuronal structure can be precisely quantified in terms of convolutions involving the individual shape of the neuron dendrites and axon. The analysis of the connectivity pattern in terms of spectral dispersion and lacunarity was also proposed and illustrated. In addition, we have shown that, by assuming a specific type of periodical boundary condition, it is possible to construct a circulant matrix whose spectrum can be conveniently calculated and used to characterize the topological properties of the neuronal structure. In order to illustrate the interplay between neuronal shape and function, we also implemented Hopfield networks having weights constrained by the adjacency matrices defined as a consequence of the individual neuronal cell geometry. The performance of such networks, quantified in terms of the overlap measurement, was shown to be strongly related to the morphology of the adopted neurons.

Although the proposed methodology assumes identical, uniformly distributed neuronal cells, it is expected that they provide a reference model for investigating real

networks characterized by a certain degree of regularity, such as some subsystems found in the retina and cortex. Preliminary corroborations of such a possibility were provided by the fact that our overlap simulations tended to be robust to small lattice perturbations. Mean-field extensions of the reported approach are currently being investigated.

This work was financially supported by FAPESP (processes 02/02504-01, and 99/12765-2 and CNPQ (process 308231/03-1).

References

1. D. Purves, J.W. Lichtman, *Principles of Neural Development* (Sinauer, 1985)
2. J. Karbowski, Phys. Rev. Lett. **86**, 3674 (2001)
3. L. da F. Costa, Special issue, Brain and Mind **4** (2003)
4. O. Shefi, I. Golding, R. Segev, E. Ben-Jacob, A. Ayali, Phys. Rev. E **66**, 021905 (2002)
5. R. Segev, M. Benveniste, Y. Shapira, E. Ben-Jacob, Phys. Rev. Lett. **90**, 168101 (2003)
6. L. da F. Costa, E.T.M. Monteiro, Neuroinformatics **1**, 065 (2003)
7. R. Albert, A.-L. Barabási, Rev. Mod. Phys. **74**(1), 47 (2002)
8. B. Bollobás, Modern Graph Theory (Springer-Verlag, New York, 2002)
9. A.L. Barabási, E. Ravasz, T. Vicsek, Physica A **299**, 564 (2001)
10. F. Buckley, F. Harary, *Distance in Graphs* (Addison-Wesley, Redwood City, 1990)
11. L.A.N. Amaral, A. Scala, M. Barthélémy, H.E. Stanley, Proc. Natl. Acad. Sci. **97**, 11149 (2000)
12. D. Stauffer, A. Aharony, L. da F. Costa, J. Adler, Eur. Phys. J. B **32**, 395 (2003)
13. L. da F. Costa, M. S. Barbosa, V. Coupez, D. Stauffer, Brain and Mind **4**, 91 (2003)
14. B.B. Boycott, H. Wassle, J. Physiol. **240**, 397 (1974)
15. C. Allain, M. Cloitre, Phys. Rev. A **44**, 3552 (1991)
16. T.G. Smith, G.D. Lange, W.B. Marks, J. Neuroci. Methods **69**, 133 (1996)
17. R.E. Plotnick, R.H. Gardner, W.W. Hargrove, K. Prestegaard, M. Perlmutter, Phys. Rev. E **53**, 5461 (1996)
18. Y. Gefen, Y. Maier, B.B. Mandelbrot, A. Ahanory, Phys. Rev. Lett. **50**, 145 (1983)
19. J.P. Hovi, A. Aharony, D. Stauffer, B. Mandelbrot, Phys. Rev. Lett. **77** (1996)
20. L. da F. Costa, *Shape analysis and classification: theory and practice* (CRC, 2001)
21. S. Haykin, *Neural Networks: A Comprehensive Foundation* (Prentice-Hall, Upper Saddle River, 1999)
22. D. Stoyan, W.S. Kendall, J. Mecke, *Stochastic Geometry and its Applications* (John Wiley and Sons, 1995)